Application of neural networks in beam emission spectroscopy modelling

M. Karacsonyi [1,2], O. Asztalos [1,2], A. Jalalvand [3], D.I. Réfy [2] and G.I. Pokol[1,2]

[1] *Budapest University of Technology and Economics, Budapest, Hungary*

[2] *Centre for Energy Research, Budapest, Hungary*

[3] *Princeton University, Princeton, NJ, USA*

Beam Emission Spectroscopy

Beam emission spectroscopy [1] (BES) is an active plasma diagnostic system in case of thermonuclear fusion plasmas, for the measurement of plasma density and density fluctuations. BES synthetic diagnostics such as RENATE [2] or RENATE-OD [3],[7] are computationally expensive and comprehensive modelling suites, designed to provide a better understanding of the diagnostic's perception of underlying plasma phenomena. RENATE-OD is an advanced BES synthetic diagnostic relying on a rate-equation solver to derive the beam emission for given input plasma profiles.

Any meaningful applications of BES synthetic diagnostics [4],[5],[6] require these calculations to be repeated $10^5 - 10^{10}$ times depending on the specific system, significantly increasing the computational time it takes to generate synthetic measurement signals.

Applying neural networks to predict the solutions of such calculations could help significantly reduce the computational time while keeping the model accuracy optimal if a sufficiently well-performing network is constructed for the task. The work presented bellow is the first step of this process, where we created a neural network which can predict the emission profiles from smooth analytical plasma density profiles.

Underlying physics, the Rate equations

The rate equations are used to describe the valance electron population of the different electron shells of the atoms of the beam which is injected into the plasma. The population of the i^{th} level is given as described below.

$$\boldsymbol{\frac{dN_i}{dx} = n_e(x)C_{ei}(T_e(x), N_i(x)) + \sum_I n_I(x)C_{Ii}(T_I(x), N_i(x)) + C_{Si}(N_i(x))}$$

Where N_i is the valence electron distribution along the beam on the i^{th} atomic level, n_e is the electron density along the beam n_I are the various ion densities along the beam, T_x are the various plasma temperature profiles of electrons and ions along the beam and n_i is the combined ion population along the beam. While C_{ei} is the electron impact collisional source term C_{Ii} is the ion impact collisional source term and C_{Si} is the spontaneous emission source term.

After calculating the valance electron population of the electron shells, the emission can be calculated by applying the corresponding Einstein coefficients.

Neural networks

We tried linear regression, single and dual-layer perceptron networks, and single and dual-layer extreme learning machines in this work.

Linear regression, being the simplest of all, uses a linear combination of the input variables with optimized weights to predict the output.

Perceptron networks are simple feed-forward neural networks, which consist of neurons. Each neuron takes the linear combination of the input variables and applies a nonlinear activation function to construct the output.

Extreme learning machines (ELMs) [8],[9] are structurally similar to perceptron networks, with the only difference being that for Extreme learning machines only the output weights are trained as shown in Figure 1. Other parameters are random initialized and fixed during training.

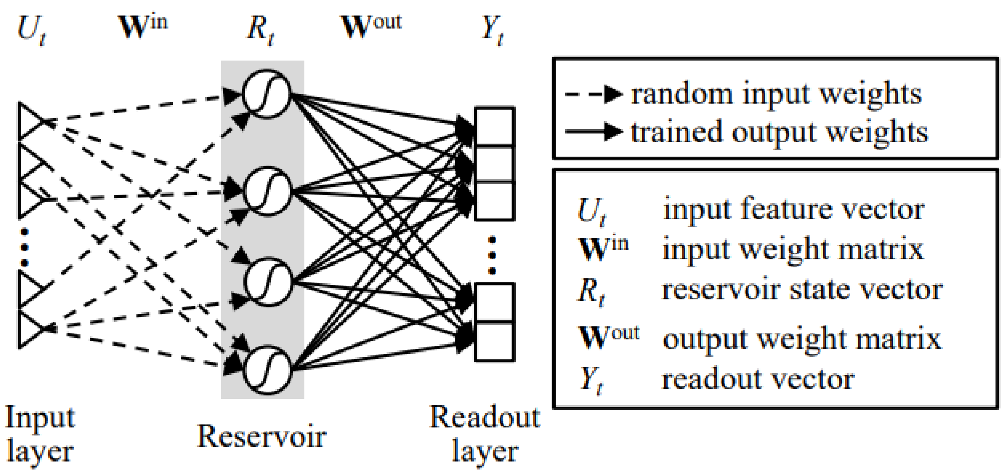

Figure 1 Architecture of a single layer Extreme learning machine

Results

We generated a synthetic dataset assuming quasi neutral pure plasma, relying on smooth idealized interpretations of plasma density profiles. The plasma density profiles were given by the following tangent hyperbolic function.

$$\rho(x) = \rho_{min} + \frac{\rho_{max} - \rho_{min}}{2} \cdot \left[1 + \tanh\left(g \cdot (x - x_0)\right)\right]$$

Where ρ_{min} is the scrape-off layer density, ρ_{max} is the pedestal top density, g is the steepness of the density profile at the inflection point and x_0 is the position of the last closed flux surface. These parameters were varied in the ranges shown in Table 1.